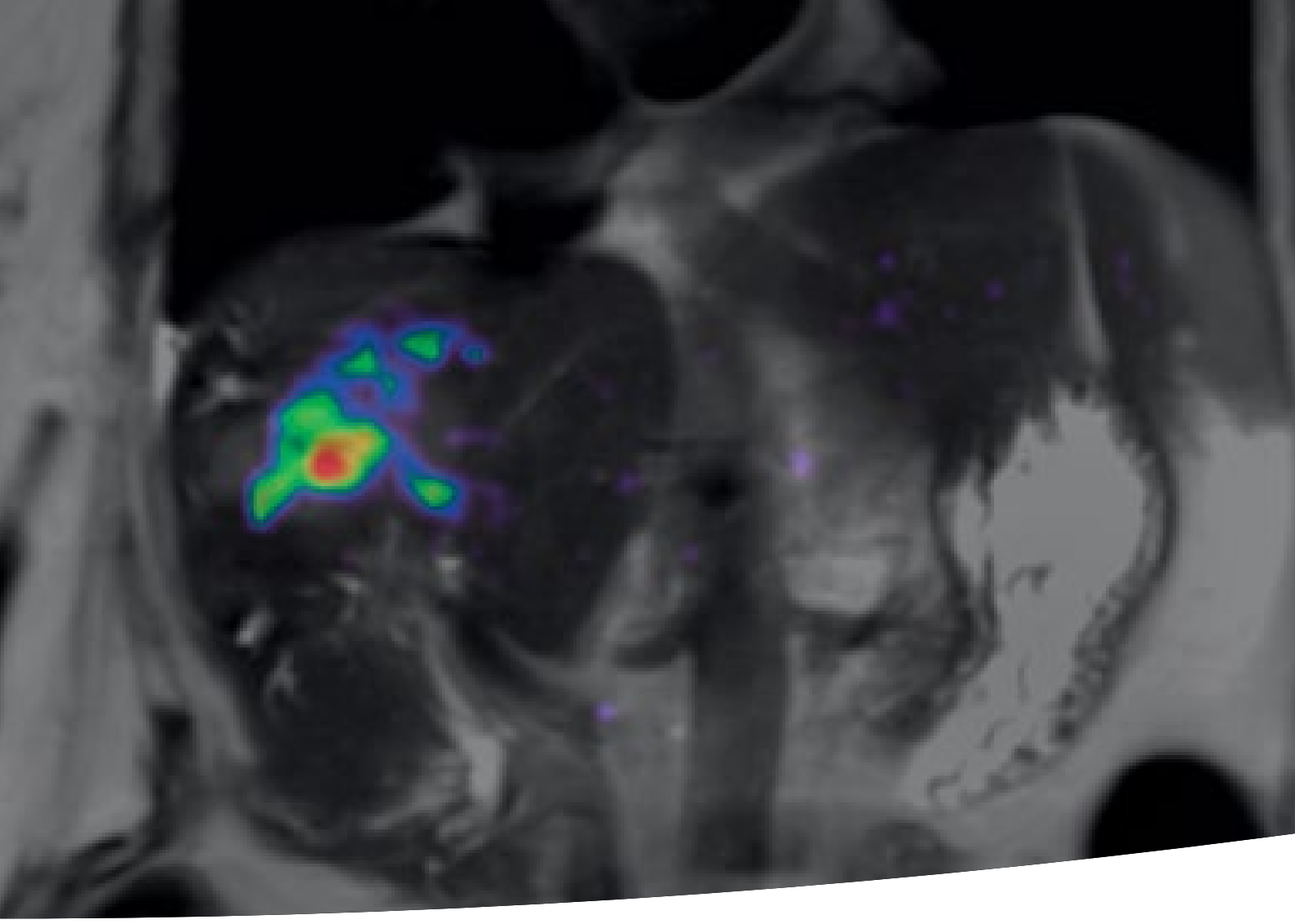

Motion Correction of ^{90}Y Dose Maps with MR/PET Imaging

usa.siemens.com/mmr

SIEMENS Healthineers

Motion Correction of ^{90}Y Dose Maps with MR/PET Imaging

Introduction

Yttrium-90 (^{90}Y)* radioembolization is a therapeutic procedure that delivers local radiation to hepatic tumors[1]. Clinically, patients undergo a ^{90}Y Bremsstrahlung SPECT scan to determine if there was any extrahepatic deposition and, most importantly, to predict if the tumor is likely to respond to therapy based on the level of the delivered dose[2]. In addition, it is also possible to image and quantify the delivered ^{90}Y dose by PET, which was shown in this study to be superior to Bremsstrahlung SPECT in terms of spatial resolution and quantification accuracy[3]. Clinical SPECT and PET scanners are currently integrated with CT systems to enable localization as well as attenuation correction of the detected emission activity signal from the CT anatomical transmission signal[4]. However, clinical PET/CT studies have shown that the relative difference in dose between responding and non-responding lesions may be as low as 25%, thus demonstrating the importance of precise anatomical localization and high quantitative accuracy when assessing dose deposition[5]. Localization of the 90Y signal distribution in the liver can be challenging with PET/CT, mainly due to the poor soft tissue discrimination and limited motion tracking capabilities offered by CT.

However, the recent advent of integrated MR/PET systems in clinic, supporting the simultaneous acquisition of PET and MR data, has enabled the automatic and highly accurate spatiotemporal co-registration of metabolic PET with anatomical and functional MR images[6]. First, MRI is associated with considerably better soft tissue constant therefore permitting the more accurate drawing of ROIs on the MR image when evaluating ^{90}Y PET regional assessments (Fig. 1). Second, the superior soft tissue resolution and absence of radiation exposure of MRI allows for more accurate tracking of the respiratory motion for improved PET motion correction. Thus, MR/PET could considerably enhance quantification in ^{90}Y dose imaging and therefore potentially improve therapeutic efficiency in clinic. Indeed, recent MR/PET studies have indicated a stronger relationship between tumor response and delivered dose even in the absence of motion correction[7]. In this study we are targeting the optimization of clinical ^{90}Y MR/PET imaging with a particular focus on MR-based motion correction of the ^{90}Y dose maps using the Biograph mMR integrated MR/PET system[8].

**Availability subject to restrictions. Agent referenced herein is not currently recognized by the US FDA as being safe and effective, and Siemens Healthineers does not make any claims regarding their use.*

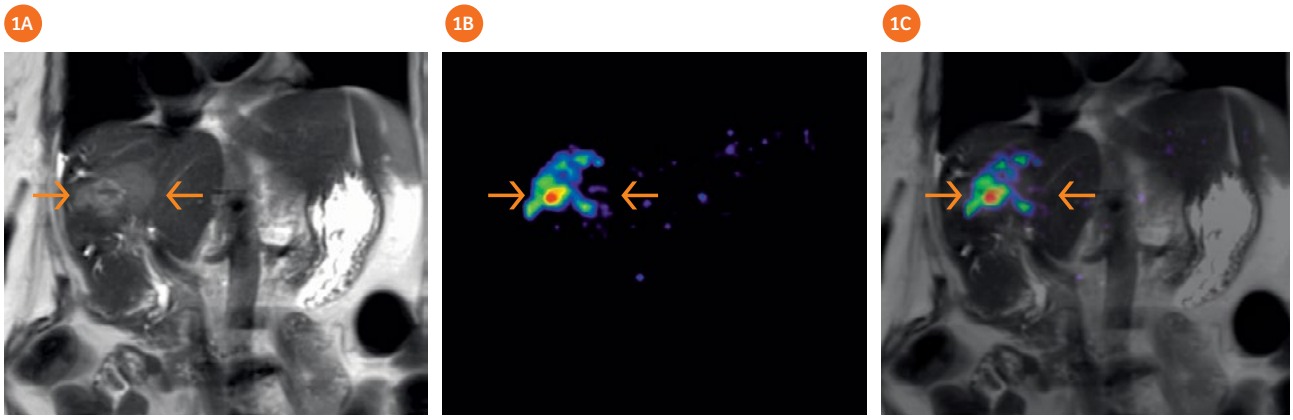

Figure 1A-C: MRI (1A), PET (1B), and fused MRI/PET (1C) images of a subject who underwent 90Y radioembolization. Arrows point to the lesion in the MR image (COR-HASTE) and the PET image.

Motion tracking and correction strategy for simultaneous ^{90}Y MR/PET imaging

The acquisition of anatomical MR signal of high spatial and temporal resolution allows for high temporal sampling rates of detailed 3D respiratory 3D cartesian motion vector field (MVF) estimates. In addition, the simultaneous acquisition of ^{90}Y PET data permits their synchronization with the MR-based respiratory motion phase for the accurate respiratory gating of the PET data. Finally, the gated PET data and the MVF are imported into a 4D PET motion-compensated image reconstruction (MCIR) algorithm to directly generate the motion-corrected ^{90}Y PET dose maps.

In this study, we exploit MR-based motion correction capabilities of the Biograph mMR system to assess the quantitative accuracy of the ^{90}Y dose distribution assessments by reducing the respiratory motion blurring effect in the final PET reconstructed images. The lesions are often in the top region of the liver, which could move up to 2 cm due to respiration[9]. Therefore, our main goals are to:

1) Develop an optimal data acquisition and reconstruction scheme specially tuned for ^{90}Y imaging post radioembolization on the Siemens Biograph mMR; and

2 **Figure 2:** Sketch of the current data acquisition protocol on the mMR at Mount Sinai. Total scan time on the horizontal direction is about 30 minutes and includes patient positioning in the scanner.

2) Evaluate the Biograph mMR motion correction algorithm (software version *syngo* MR E11p).

Previously, we conducted a preliminary evaluation of the MCIR algorithm performance on ^{90}Y phantom studies[10,11]. Currently, we expand our validation on patient data to optimize the motion-compensated reconstruction parameters in the clinic.

Our current protocol at Mount Sinai is outlined in Figure 2. The total scan time ranges between 30 and 35 minutes. Currently we run a prototype motion tracking sequence** (Siemens BodyCOMPASS) during the acquisition of the PET scan. The sequence permits the generation of a set of high resolution 3D MR gated images, namely a 4D MR image, each corresponding to a different phase of the respiratory cycle, from end-expiration to end-inspiration. Subsequently, standard image registration methods are used to calculate from the gated MR images the 3D non-rigid motion transformation maps, which constitute the estimated motion model. In addition, the same MR data can be utilized to track the trace of the respiratory motion throughout the PET acquisition. This trace can be later employed to sort the synchronized PET data into the same set of respiratory gates. After the completion of the MR tracking sequence, we acquire additional MRI data with sequences designed for high-resolution anatomical static imaging to facilitate the accurate MR-based region-of-interest (ROI) localization in the ^{90}Y PET dose maps. Current MRI sequences in the exam are: 1) Axial HASTE, 2) Coronal HASTE, 3) 3D Dixon, 4) Axial T1w. We find HASTE images to be best for that purpose; however, contrast-enhanced MRI is used by other groups and its use should be investigated in the future. It is important to note that

***AWIP, the product is currently under development and is not for sale in the US and in other countries. Its future availability cannot be ensured.*

3A 3B 3C

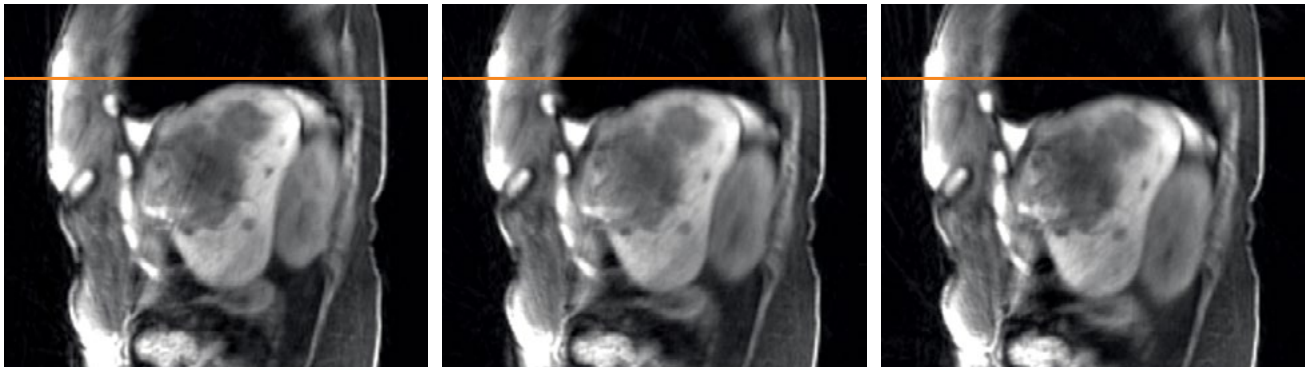

Figure 3A-C: Examples of 3 different MR gated images corresponding to respective phases of the respiratory motion cycle, as generated with MR motion tracking sequence included in Biograph mMR *syngo* MR E11p software.

for ^{90}Y imaging it would be ideal to find only one sequence to be used for ROI definition in order to minimize scan time as much as possible. As a consequence, it would then be feasible to dedicate the entire PET scan for motion tracking if needed.

Figure 3 shows sample sagittal images showing the various phases. The sequence as well as the data sorting algorithm seems to perform well in resolving motion.

Enhancing ^{90}Y dose maps quantification with motion-compensated MR/PET imaging

Figure 4A illustrates a clear visual improvement in resolution and contrast of ^{90}Y dose maps after application of motion correction within the PET reconstruction. Motion corrected ^{90}Y PET images (right) are characterized by higher signal contrast recovery compared to the respective images without motion correction, i.e. static images (left). Moreover, the motion-corrected ^{90}Y images are associated with superior signal-to-noise ratio (SNR) compared to the gated ^{90}Y image (middle). The line plot in Figure 4B quantitatively confirms the improved contrast recovery for ^{90}Y dose maps when motion correction is applied. The degree of ^{90}Y contrast enhancement in the liver would be expected to reach maximum score levels for lesions located in the top of the liver, at the liver-lung interface. This is attributed to the strongest resolution degradation effects often observed in the liver-lung interface due to respiratory motion-induced contamination of the liver ^{90}Y uptake signal with the considerably smaller background signal from the lung. Indeed, the alignment of the ^{90}Y dose with the MR anatomical map before and after motion correction in Figure 5 illustrates the automatic correction of the position of the ^{90}Y deposited dose distribution within the liver after motion correction. This is of high importance in clinical practice, as occasionally a percentage of ^{90}Y activity may be observed in lungs due to air embolization[12].

Furthermore, in Figure 6 more clinical cases are presented where reconstructed 90Y dose maps have benefited from MR-based PET motion correction. The contrast recovery enhancement of motion-corrected versus static PET images is visually evident in focal ^{90}Y uptake regions.

Moreover, in some clinical cases, no attachment to the target was observed for the delivered ^{90}Y dose thus resulting in diffused ^{90}Y distribution as shown in Figure 7. Nevertheless, the Biograph mMR *syngo* MR E11p motion correction algorithm did not induce any artifacts or false positives.

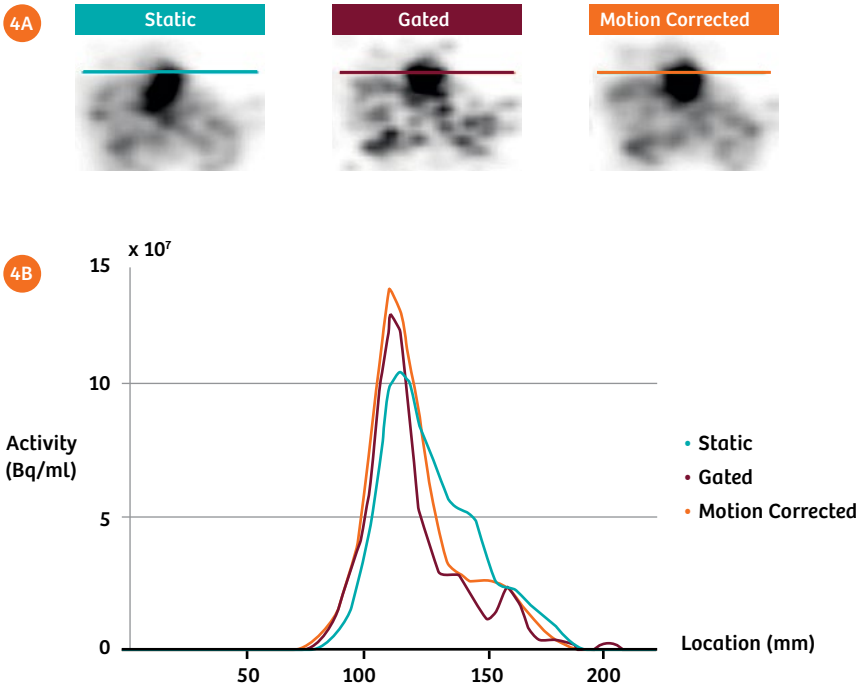

Figure 4A-C: (4A) ^{90}Y PET images reconstructed without motion correction (static), gated (i.e. using the acquired data from only one respiratory phase), or motion corrected. Motion correction clearly improves activity signal recovery as shown visually in PET images **(4A)** and quantitatively in the respective line profiles **(4B)**.

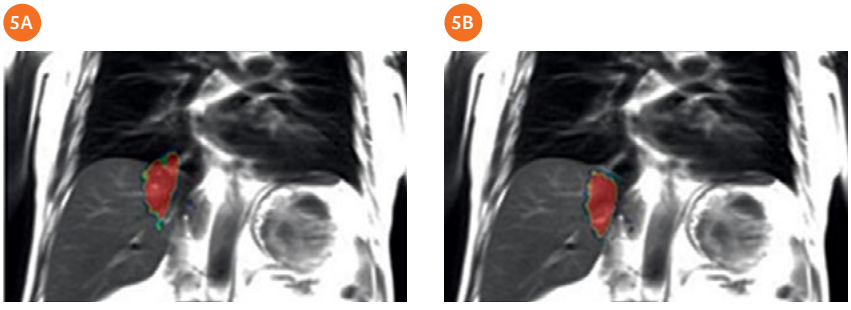

Figure 5A-B: Automatic co-registration of MR with ^{90}Y before **(5A)** and after **(5B)** PET motion correction demonstrating the significantly improved accuracy in localizing the ^{90}Y signal distribution after motion correction.

Clinical prospects in motion-compensated ^{90}Y MR/PET imaging

Our preliminary findings in a few patients show that MR based motion correction for ^{90}Y could improve the quantitative accuracy of the data. As mentioned above, the literature indicates a difference between responding and non-responding lesions of 25%, and thus the margin for error is quite small. The effect of motion, especially at the top of the liver, could be higher than that margin and thus its use could be significant. To accurately measure the improvement, a cohort of about 20-30 subjects is desirable to show the potential benefits of motion correction. There are some attenuation correction issues including lack of a lung segment (i.e. LAC = 0) in some of our cases which require further evaluation. We have been using the motion correction sequence using the default parameters and this might require some optimization. Moreover, optimization, streamlining, and integration of motion correction into routine reconstruction are needed. Finally, the best number of gates and the navigator signal from the belt should be further investigated.

Contact
Zahi A. Fayad, Ph.D, FAHA,
zahi.fayad@mssm.edu

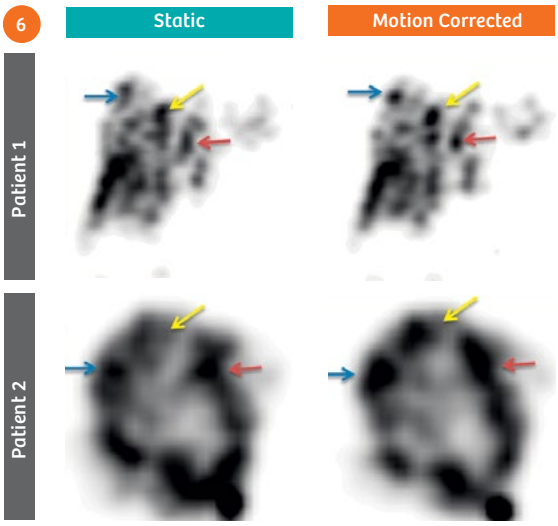

Figure 6: Clinical ^{90}Y PET images without (static) and with motion correction for 2 clinical cases with specific binding of ^{90}Y to the liver tissue.

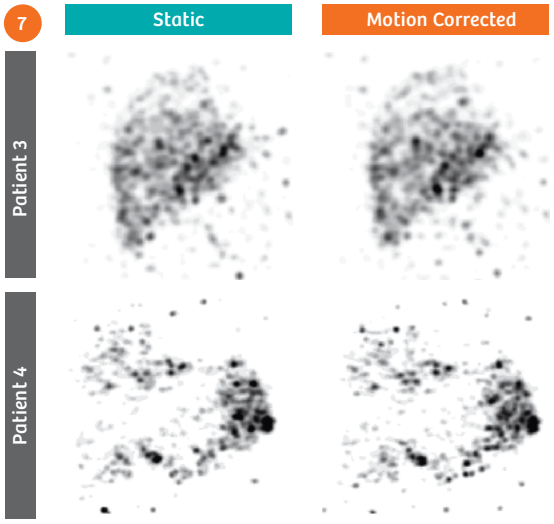

Figure 7: Clinical ^{90}Y PET images without (static) and with motion correction for 2 clinical cases characterized by absence of specific binding of ^{90}Y to the liver tissue.

Authors

Nicolas A. Karakatsanis, Ph.D., MEng
Translational and Molecular Imaging Institute
Icahn School of Medicine at Mount Sinai
New York, NY, USA

Mootaz Eldib, Ph.D.
Translational and Molecular Imaging Institute
Icahn School of Medicine at Mount Sinai
New York, NY, USA

Niels Oesingmann, Ph.D.
Siemens Healthineers, New York, NY, USA

David D. Faul, Ph.D.
Siemens Healthineers, New York, NY, USA

Lale Kostakoglu, MD, MPH
Department of Radiology
Icahn School of Medicine at Mount Sinai
New York, NY, USA

Karin Knesaurek, Ph.D.
Department of Radiology
Icahn School of Medicine at Mount Sinai
New York, NY, USA

Zahi A. Fayad, Ph.D.
Translational and Molecular Imaging Institute
Icahn School of Medicine at Mount Sinai
New York, NY, USA

Cardiovascular Institute
Icahn School of Medicine at Mount Sinai
New York, NY, USA

References

[1]Salem R and Thurston KG. Radioembolization with 90 Yttrium microspheres: a state-of-the-art brachytherapy treatment for primary and secondary liver malignancies: part 1: Technical and methodologic considerations. Journal of vascular and interventional radiology 2006; 17: 1251-1278.

[2]Sarfaraz M, Kennedy AS, Lodge MA, Li XA, Wu X and Cedric XY. Radiation absorbed dose distribution in a patient treated with yttrium-90 microspheres for hepatocellular carcinoma. Medical physics 2004; 31: 2449-2453.

[3]Elschot M, Vermolen BJ, Lam MG, de Keizer B, van den Bosch MA and de Jong HW. Quantitative comparison of PET and Bremsstrahlung SPECT for imaging the in vivo yttrium-90 microsphere distribution after liver radioembolization. PLoS One 2013; 8: e55742.

[4]Townsend DW, Carney JP, Yap JT and Hall NC. PET/CT today and tomorrow. Journal of Nuclear Medicine 2004; 45: 4S-14S.

[5]Srinivas SM, Natarajan N, Kuroiwa J, Gallagher S, Nasr E, Shah SN, DiFilippo FP, Obuchowski N, Bazerbashi B, Yu N and McLennan G. Determination of Radiation Absorbed Dose to Primary Liver Tumors and Normal Liver Tissue Using Post-Radioembolization (90)Y PET. Front Oncol 2014; 4: 255.

[6]Judenhofer MS, Wehrl HF, Newport DF, Catana C, Siegel SB, Becker M, Thielscher A, Kneilling M, Lichy MP and Eichner M. Simultaneous PET-MRI: a new approach for functional and morphological imaging. Nature medicine 2008; 14: 459-465.

[7]Fowler KJ, Maughan NM, Laforest R, Saad NE, Sharma A, Olsen J, Speirs CK and Parikh PJ. PET/MRI of hepatic 90Y microsphere deposition determines individual tumor response. Cardiovascular and interventional radiology 2016; 39: 855-864.

[8]Delso G, Fürst S, Jakoby B, Ladebeck R, Ganter C, Nekolla SG, Schwaiger M and Ziegler SI. Performance measurements of the Siemens mMR integrated whole-body PET/MR scanner. Journal of nuclear medicine 2011; 52: 1914-1922.

[9]Osman MM, Cohade C, Nakamoto Y and Wahl RL. Respiratory motion artifacts on PET emission images obtained using CT attenuation correction on PET-CT. European journal of nuclear medicine and molecular imaging 2003; 30: 603-606.

[10]Maughan NM, Eldib M, Conti M, Knešaurek K, Faul D, Parikh PJ, Fayad ZA and Laforest R. Phantom study to determine optimal PET reconstruction parameters for PET/MR imaging of 90Y microspheres following radioembolization. Biomedical Physics & Engineering Express 2016; 2: 015009.

[11]Eldib M, Oesingmann N, Faul DD, Kostakoglu L, Knešaurek K and Fayad ZA. Optimization of yttrium-90 PET for simultaneous PET/MR imaging: A phantom study. Medical Physics 2016; 43: 4768-4774.

[12]Herba M, Illescas F, Thirlwell M, Boos G, Rosenthall L, Atri M and Bret P. Hepatic malignancies: improved treatment with intraarterial Y-90. Radiology 1988; 169: 311-314.

On account of certain regional limitations of sales rights and service availability, we cannot guarantee that all products included in this brochure are available through the Siemens Healthineers sales organization worldwide. Availability and packaging may vary by country and is subject to change without prior notice. Some/All of the features and products described herein may not be available in the United States.

The information in this document contains general technical descriptions of specifications and options as well as standard and optional features, which do not always have to be present in individual cases.

Siemens Healthineers reserves the right to modify the design, packaging, specifications, and options described herein without prior notice. For the most current information, please contact your local sales representative from Siemens Healthineers.

Note: Any technical data contained in this document may vary within defined tolerances. Original images always lose a certain amount of detail when reproduced.

Siemens Healthineers Headquarters
Siemens Healthcare GmbH
Henkestr. 127
91052 Erlangen, Germany
Phone: +49 9131 84-0
siemens-healthineers.com

Local Contact Information
Siemens Medical Solutions USA, Inc.
40 Liberty Boulevard
Malvern, PA 19355-9998, USA
Phone: 1-888-826-9702
siemens-healthineers.us

Order No. 24-18-11362-01-76 · Printed in USA · 05-2018 · *©Siemens Medical Solutions USA, Inc., 2018*